Wakefield Accelerator Driven to Ionisation Injection Using a Laser Reflected Off a Plasma Mirror at High Intensities

Contact: jasmin.hills19@ic.ac.uk

J. Hills, M. P. Backhouse, R. Luo, L. Kennedy, C. Cobo, E. Los, Z. Najmudin
Blackett Laboratory, Imperial College London, SW7 2BZ, United Kingdom

E. Gerstmayr, J. Sarma
Queen's University Belfast, Belfast, BT7 1NN, United Kingdom

P. Blum
Deutsches Elektronen-Synchrotron DESY, Notkestr. 85, 22607 Hamburg, Germany

N. Lopes
Instituto de Plasmas e Fusão Nuclear, Instituto Superior Tecnico, Universidade de Lisboa, 1049-001 Lisbon, Portugal

N. Bourgeois
Central Laser Facility, STFC Rutherford Appleton Laboratory,Oxfordshire, OX11 0QX, United Kingdom

Abstract

We report on a laser wakefield accelerator driven to ionisation injection using a laser pulse reflected from a pellicle plasma mirror operating at high intensities. Reflected pulses containing a maximum total energy of 3.2 ± 0.9 J were used to demonstrate a guided central spot at densities exceeding $0.5 \times 10^{24}\,\mathrm{m}^{-3}$. Entire blue shifting of the transmitted pulse was observed between $0.5 \times 10^{24}\,\mathrm{m}^{-3}$ and $2 \times 10^{24}\,\mathrm{m}^{-3}$. Ionisation injection was demonstrated with spots containing up to 0.4 ± 0.1 J in their FWHM at densities exceeding $2.7 \pm 0.4 \times 10^{24}\,\mathrm{m}^{-3}$. Electrons were accelerated in a cell of $6.7 \pm 0.8 \times 10^{24}\,\mathrm{m}^{-3}$ to energies up to 455 ± 28 MeV using the reflected pulse. The results presented here support the utility of a tape-based plasma mirror for driving the second stage of a wakefield accelerator.

1 Introduction

The use of multiple acceleration stages may be necessary to reach high energies through laser wakefield acceleration. This concept, referred to as staging, lines up multiple wakefield accelerators such that an electron beam injected and accelerated in one stage is transported to the accelerating region of the next. Staging offers a method of circumventing the depletion of driving laser energy by coupling in a second laser beam. Coupling in this pulse, whilst maintaining a high average accelerating gradient, requires the use of optics at high intensities. Conventional optical components cannot be used near focus, as this would result in fluence above their damage threshold. Moving the coupling optics away from focus, to intensities below this threshold, would increase the coupling distance, L_c, and complicate electron beam transport between cells [1], reducing the overall acceleration gradient.

The use of plasma mirrors can reduce the coupling distance [2] but may degrade the quality of the reflected pulse and the energy contained within the FWHM [3, 4]. Efficient laser wakefield acceleration requires a high fraction of energy within the FWHM, meaning that poor reflection quality reduces the attractiveness of staging. The use of plasma mirrors to achieve staging was demonstrated by the team at LBNL in 2016, where 3 % of a LWFA generated beam was captured and accelerated by 100 MeV [5]. Higher energy gain and charge capture will be required for staging to be feasible. Being able to couple in a high intensity pulse over a short distance is fundamental to both of these aims.

The plasma mirror reflected pulse is respon-

sible for generating a wakefield in the second stage. The properties of this reflected pulse determine the properties of the wakefield including the density threshold at which self-guiding and injection occur.

To observe reasonable energy gain the laser pulse must maintain a high enough intensity to generate accelerating fields over distances exceeding the Rayleigh length. Laser diffraction can be prevented through self-focusing, intense laser pulses induce a change in local refractive index, generating a refractive index gradient that results in wavefront curvature and focussing. The extent of this focussing behaviour depends on the initial plasma density. The self-guiding threshold is the density at which this focussing balances out laser diffraction. This density provides a lower bound for the suitable operating range for external injection.

The charge capture and energy gain of externally injected beams is improved by using low densities. This increases the size of the accelerating structure ($\lambda_p \propto n_e^{-1}$) and energy gain ($W_{gain} \propto n_e^{-1}$), where λ_p is the wavelength of the generated plasma waves. But larger structures require more laser energy to drive them. As a result operating as close to this lower density threshold as possible may be beneficial for optimising external injection in staging.

The injection threshold is the density at which plasma electrons become trapped in the focussing and accelerating part of the wave. The onset of injection provides an upper limit to the operating range for external injection, as injection of this type during staging will ruin beam quality of the externally injected beam. This threshold can be used to determine the quality of the reflected pulse, as it is sensitive to the energy contained within the FWHM. This is because the laser spot is focused by the plasma to the order of $\lambda_p = 2\pi c/\omega_p$. Higher densities result in a smaller λ_p, this reduced spot size increases the pulses intensity. A high enough density plasma can focus a spot to an intensity above the required field strengths for injection. This required field strength can be lowered through the use of a dopant, chosen to have bound electrons that are ionised within the wakefield. Ionisation of the dopant inner shell electrons occurs close to the peak of the driving laser pulse, which is inside the wakefield. For sufficiently large wakefield amplitudes these ionised electrons can become trapped [6].

Here, pulses reflected from a high intensity plasma mirror were used to drive a wake across different gas cell densities. The operating range over which this pulse could be used for external injection was determined. The utility of these pulses for staging applications was demonstrated through evidence of guiding, ionisation-injection and subsequent acceleration of these self-ionisation-injected electrons to energies of 455 MeV .

2 Experimental Methods

These investigations utilised the GEMINI North beam, an 800 nm s-polarised pulse with energies between 1-15 J in a duration of $\sim$ 50 fs. A 7500 mm focal distance dielectric spherical mirror focused the beam from a diameter of 150 mm to a focal spot size of $\sim$ 50 μm. An adaptive optic was used in conjunction with a Shack-Hartmann wavefront sensor, an *Imagine Optics HASO*, to flatten the wavefront. This input pulse was focused 9.0 ± 1.5 mm after a tape-based plasma mirror and characterised before the introduction of a gas cell, as described in [7]. The plasma mirror was generated through the ionisation of Kapton tape. A tape drive was used to tension and replenish this tape. The tape drive was adjusted to point the reflected north beam onto the optical axis of the gas cell.

Run	**A**	**B**
Energy (J)	3.2(0.9)	4.5(1)
Energy in FHWM (J)	0.2(0.1)	0.4(0.1)

Table 1: Energy contained within the highest energy and strehl ratio reflected spots for the Guiding (A) and Injection (B) density scans.

Before the gas cell was introduced, the input pulses reflected from the plasma mirror were

characterised using the forward line diagnostics described in [7]. The mirror was characterised to produce reflectivities in excess of 70% across a broad range of intensities (from $1 \times 10^{20}\,\mathrm{W/m^2}$ to $5 \times 10^{21}\,\mathrm{W/m^2}$). The plasma mirror had an average reflectivity of $50.0 \pm 8.0\,\%$ at the intensities utilised in the injection scan (B), and $41.0 \pm 3.0\,\%$ for the density scan (A). The highest energies and pulse profiles from these scans are presented in table 1. More energy was coupled into the laser spots during the injection density scan (B), with a higher overall reflectivity and ratio of energy in the FWHM.

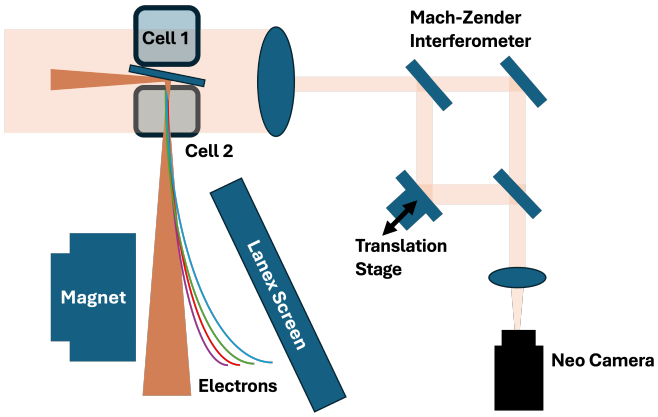

Figure 1: The set-up in GEMINI TA3, including electron spectrometer and interferometry probe of cell 1 and cell 2.

A gas cell could be driven in and out of the path of the reflected laser. The gas consisted of helium with 2% nitrogen dopant to enable ionisation injection. Different cell lengths were utilised for different runs with 23 mm and 10 mm used for guiding (A) and injection (B) respectively. Control over the gas pressure allowed for the varying of cell densities. The gas cells were fitted with glass windows for observation of the plasma. A leakage from the drive beam was taken as a probe, and timed to allow imaging of the plasma channel immediately after formation. A Mach-Zender interferometer was used to determine the plasma density. Uncertainties were given by the standard deviation of the measured density. An Au-spherical mirror was used to image the end of the gas cell on the far-field camera and transmit energy to a Gentec QE8SP-B-BL-D0 energy meter outside the vacuum chamber. This calorimeter was calibrated to measure energy at target chamber centre (details in [7]). An OceanOptic NIRquest spectrometer characterised the transmitted lasers' spectrum.

A permanent dipole magnet was driven onto the beam axis to deflect electrons injected in the gas cell to a series of Lanex screens at different distances, as in figure 1. A mid-energy spectrometer, covering between 100 MeV and 2300 MeV, was used for the results presented here (for more details see [8]).

3 Guiding and Transmitted beams

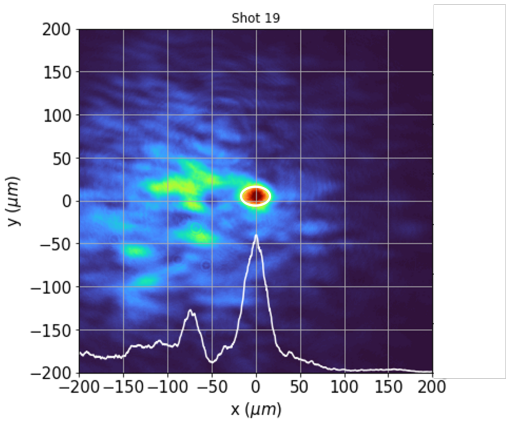

Figure 2: Typical image of transmitted laser energy during the guiding scan, at a density of $1 \times 10^{24}\,\mathrm{m^{-3}}$. The central guided spot is fitted with a white ellipse, from which the FWHM is extracted. An intensity line-out is plotted on a parallel axis.

A density scan was performed to determine the guiding properties of the reflected pulse using a 23 mm cell and the input pulse described in table 1 (A). A guided central spot was observed at densities between $0.5 \times 10^{24}\,\mathrm{m^{-3}}$ and $2 \times 10^{24}\,\mathrm{m^{-3}}$, an example image is shown in figure 2. The FWHM contour of the transmitted spots were fitted with ellipses. The size of these ellipses is plotted against the expected plasma wave wavelength, λ_p, for a given density. This

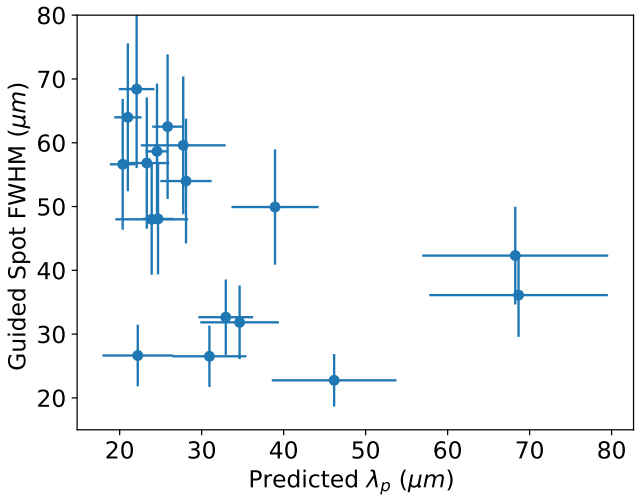

Figure 3: Plasma wavelengths, $\lambda_p \approx 2\pi c/w_p$, inferred from measured densities against measured guided spot FWHM.

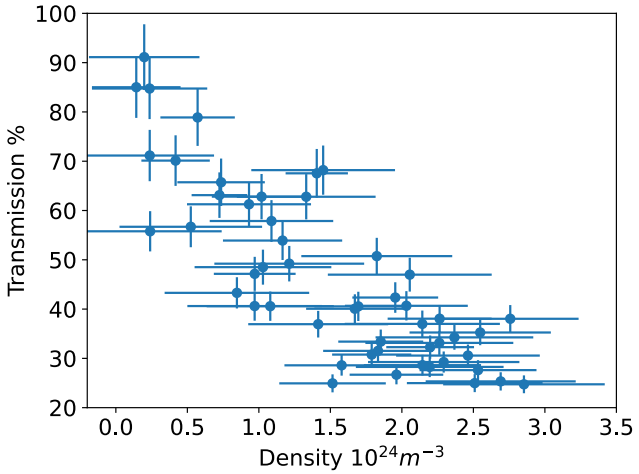

Figure 4: Transmission through the gas cell compared to the incident laser energy after reflection (assuming reflectivity of $41.0 \pm 3.0\,\%$). Measurements were taken at the end of a 23 mm gas cell for varying density.

density was measured using interferometry. It is expected that these two would be correlated as the plasma should focus the reflected spot down to the plasma wave wavelength. However, as shown in figure 3, the correlation is poor. The measured average ellipse widths varied between 20 and 70 μm, corresponding to densities of $0.2 \times 10^{24}\,\mathrm{m}^{-3}$ and $0.8 \times 10^{24}\,\mathrm{m}^{-3}$. Most of the measured spots are larger than expected at the relevant densities. This is especially the case at higher density (small λ_p) suggesting poor guiding in these cases. In this case it appears as if the laser has not been guided over the whole cell length.

Figure 4 shows the transmitted energy through the gas cell, given by the ratio of the laser energy incident on the cell to the calorimeter measurements. The incident laser energy was approximated using the pre-reflection laser energy multiplied by the plasma mirror reflectivity ($41.0 \pm 3.0\,\%$). Transmission through the gas cell fell as the density increased. Beyond densities of $2 \times 10^{24}\,\mathrm{m}^{-3}$, no central spot was observed on the far-field camera, this is consistent with the measured transmitted spots size increasing at low λ_p. These measurements suggest that the laser has been severely depleted and so the laser has fallen below the power for self-guiding.

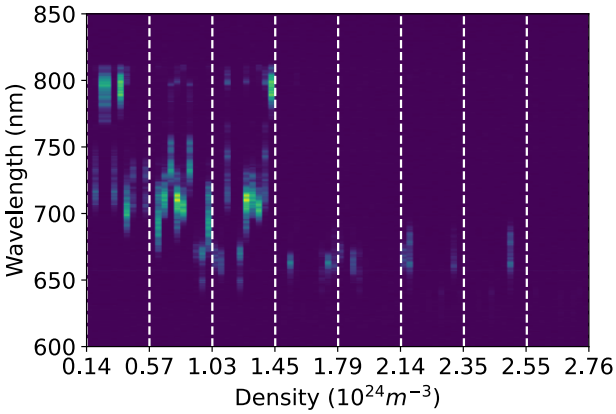

Figure 5: Measured driving laser spectrum at the end of gas cell, plotted alongside the density of the gas cell for each shot.

Figure 5 shows the measured spectra of the driving pulse, after passing through the gas cell. For most shots, at densities exceeding $0.57 \times 10^{24}\,\mathrm{m}^{-3}$, almost the entirety of the pulse was blue shifted. Blueshifting could be due to ionisation, especially for unguided light. However, it can also be caused by photon acceleration at the back of a wakefield [9][10][11], thus indicating wakefield generation. Hence it could be a signature of wakefield generation. The cor-

responding red-shift at the front of the pulse is unlikely to be seen on our spectrometer[12][13].

4 Injection Driven by Reflected Pulse

The injection thresholds were found through cell density scans using a 10 mm long cell, with incident spots described in table 1 column B. Figure 6 shows integrated electron spectra from the mid-energy spectrometer arranged in order of density. Injection occurs sporadically at densities exceeding $2.7 \pm 0.4 \times 10^{24}\,\mathrm{m}^{-3}$ until a density of around $5.6 \times 10^{24}\,\mathrm{m}^{-3}$, at which point consistent electron beams are produced, as evident in figure 6. The initial threshold is agreed upon by the low energy electron spectrometer which captured electrons between 0 and 100 MeV.

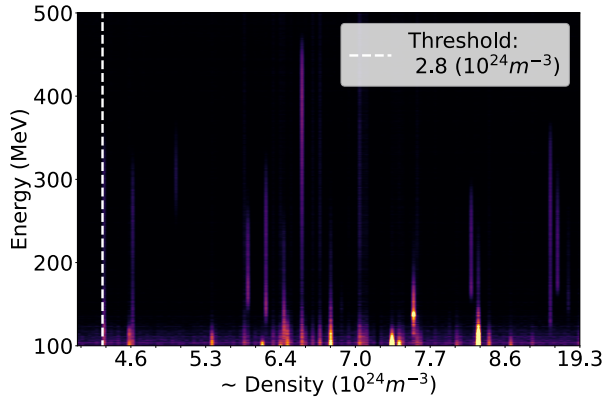

Figure 6: Density scan of electron spectra (on mid-energy spectrometer) at different cell densities with a 10mm long cell. Densities here are arranged in ascending order but have large uncertainties.

This is the first observation of a wakefield driven to the threshold for ionisation injection using a pulse reflected from a plasma mirror. These beams were observed to be accelerated up to energies of 455 ± 28 MeV with 1.2 ± 0.2 pC of charge between $100 - 455$ MeV, as in figure 7. This occurred just above the injection threshold at a density of $6.7 \pm 0.8 \times 10^{24}\,\mathrm{m}^{-3}$. At densities exceeding this peak energy a drop in measured electron energies was observed, as expected due to dephasing [14]. Figure 8 illustrates the fall in

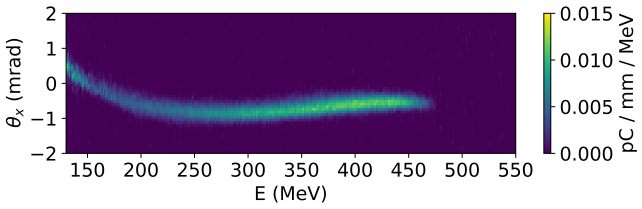

Figure 7: Example electron beam from mid-energy spectrometer with maximum energy of 455 ± 28 MeV, with 1.2 ± 0.2 pC of charge between $100 - 455$ MeV. This beam was generated at a density of $6.7 \pm 0.8 \times 10^{24}\,\mathrm{m}^{-3}$.

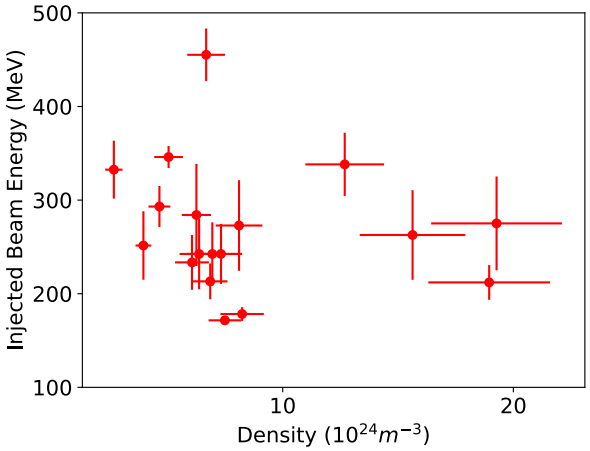

Figure 8: Density scan showing falling electron energies with increasing density.

maximum electron energy with increasing density.

5 Discussion

Considering the total reflected laser energy of 3.2 ± 0.9 J, the critical threshold for guiding, using $P_c \approx 17.5\omega_L^2/\omega_p^2$ GW [15], would be reached at $0.48 \times 10^{24}\,\mathrm{m}^{-3}$. A guided central spot was observed on the far field imaging system near the threshold predicted for this total reflected energy, i.e. $0.5 \times 10^{24}\,\mathrm{m}^{-3}$. The central mode of the guided laser pulse should be the plasma wave wavelength, i.e. $w_{FWHM} \approx \lambda_p = 2\pi c/\omega_p$. Thus for densities between 0.5-2 $\times\, 10^{24}\,\mathrm{m}^{-3}$, a wake of size comparable to scale length λ_p =20-50 μm should have been generated. The observed transmitted spot sizes exceeded this scale

over most of the density range explored. It is likely the guided pulse diffracted before the end of the cell, resulting in the expansion of the guided spot before imaging.

Considering only the energy in the central spots as causing injection, the threshold densities for ionisation injection can be estimated. The ionisation threshold for inner shell nitrogen electrons requires field strengths exceeding $E_{max} > 0.8 \times 10^{13}\,\mathrm{Vm}^{-1}$ [16][17]. For a pulse containing 0.4 J (from table 1 (B)) to exceed E_{max} the spot size must be 11.5 μm. For a pulse guided with $w = \lambda_p$ this is achieved at a density of $8.5 \times 10^{24}\,\mathrm{m}^{-3}$. Injection occurred at a lower threshold than predicted, 'turning on' at values exceeding $2.7 \pm 0.4 \times 10^{24}\,\mathrm{m}^{-3}$.
Given the input laser energies, the model by Lu et al.[18] can be used to predict the maximum electron energies that can be generated, $\Delta W/mc^2 = a_0^2 \frac{w_0^2}{w_p^2}$. Considering a pulse containing 0.4 ± 0.1 J at a density of $6.7 \pm 0.8 \times 10^{24}\,\mathrm{m}^{-3}$, once again assuming the pulse is guided with $w = \lambda_p$ a maximum electron energy of 96 MeV can be generated. It may be that this unaccounted for energy gain originates from pre-injection pulse evolution. The contribution of energy outside the FWHM to injection may explain the high maximum electron energies observed [19]. A number of the measured spectra were in a more reasonable energy range for their respective densities, its possible variation in spot quality and increased energy in the FWHM may partially account for these high energies. A total energy of 4.5 ± 0.1 J was reflected from the plasma mirror with less than 10 % contained within the FWHM. The scaling also assumed a laser spot size that doesn't evolve non-linearly during propagation, longitudinal amplification may result in an underestimate of a_0. Pulse evolution is a highly non-linear process, and requires further investigations via Particle In Cell (PIC) simulations. Further investigations and simulations of this behaviour are being performed to determine the source of this high energy gain.

References

[1] Carl A. Lindstrøm. Staging of plasma-wakefield accelerators. *Physical Review Accelerators and Beams*, 24(1), Jan 2021.

[2] B H Shaw, S Steinke, J. van Tilborg, and W P Leemans. Reflectance characterization of tape-based plasma mirrors. *Physics of Plasmas*, 23(6), Jun 2016.

[3] G G Scott, V Bagnoud, C Brabetz, R J Clarke, J S Green, R I Heathcote, H W Powell, B Zielbauer, T D Arber, P McKenna, and D Neely. Optimization of plasma mirror reflectivity and optical quality using double laser pulses. *New Journal of Physics*, 17(3):033027–033027, Mar 2015.

[4] Douglass Schumacher. Plasma mirrors for high power lasers: A new approach for high repetition rates combined with realistic pic simulations, Jun 2022.

[5] S Steinke, J. van Tilborg, C Benedetti, R Geddes, C B Schroeder, J Daniels, K K Swanson, A J Gonsalves, K Nakamura, N H Matlis, B H Shaw, E Esarey, and W P Leemans. Multistage coupling of independent laser-plasma accelerators. *Nature*, 530(7589):190–193, Jan 2016.

[6] Min Chen, Zheng-Ming Sheng, Yan-Yun Ma, and Jie Zhang. Electron injection and trapping in a laser wakefield by field ionization to high-charge states of gases. *Journal of Applied Physics*, 99(5), Mar 2006.

[7] J Hills, M Backhouse, R Luo, and Z Najmudin. Plasma mirror operation at high intensity: Reflectivity and beam profile, 2025. (ibid).

[8] M Backhouse, R Luo, J Hills, and Z Najmudin. Beam driven electron acceleration to 4 gev at gemini, 2025. (ibid).

[9] Hideyuki Kotaki, Yukio Hayashi, Michiaki Mori, Masaki Kando, James K Koga,

and Sergei V Bulanov. Limitation of the plasma channel due to the frequency blueshift. *Journal of Physics Conference Series*, 688:012054–012054, Mar 2016.

[10] S Karsch, J Osterhoff, A Popp, T P Rowlands-Rees, Zs Major, M Fuchs, B Marx, R Hörlein, K Schmid, L Veisz, S Becker, U Schramm, B Hidding, G Pretzler, D Habs, F Grüner, F Krausz, and S M Hooker. *New Journal of Physics*, 9(11):415–415, Nov 2007.

[11] R.T Sandberg and A.G.R Thomas. Photon acceleration from optical to xuv. *Physical Review Letters*, 130(8), Feb 2023.

[12] M.J.V. Streeter, Y. Ma, B. Kettle, S.J.D. Dann, E. Gerstmayr, F. Albert, N. Bourgeois, S. Cipiccia, J.M. Cole, I. Gallardo González, A.E. Hussein, D.A. Jaroszynski, K. Falk, K. Krushelnick, N. Lemos, N.C. Lopes, C. Lumsdon, O. Lundh, S.P.D. Mangles, and Z. Najmudin. Characterization of laser wakefield acceleration efficiency with octave spanning near-IR spectrum measurements. *Physical Review Accelerators and Beams*, 25(10), Oct 2022.

[13] C D Murphy, R. Trines, J Vieira, W Reitsma, R Bingham, J L Collier, E J Divall, P S Foster, C J Hooker, A J Langley, P A Norreys, R A Fonseca, F. Fiuza, L O Silva, J T Mendonça, W B Mori, J G Gallacher, R. Viskup, D A Jaroszynski, and D Mangles. Evidence of photon acceleration by laser wake fields. *Physics of Plasmas*, 13(3), Mar 2006.

[14] M.S Bloom, M.J.V Streeter, S Kneip, R.A. Bendoyro, O. Cheklov, J.M Cole, A. Döpp, C.J Hooker, J Holloway, J Jiang, N.C Lopes, H Nakamura, P.A. Norreys, P.P. Rajeev, D.R Symes, J Schreiber, J.C Wood, M Wing, Z. Najmudin, and S.P.D Mangles. Bright x-ray radiation from plasma bubbles in an evolving laser wakefield accelerator. *Physical Review Accelerators and Beams*, 23(6), Jun 2020.

[15] R Geddes, Cs Toth, J. van Tilborg, E Esarey, C B Schroeder, D. Bruhwiler, C. Nieter, J Cary, and W P Leemans. High-quality electron beams from a laser wakefield accelerator using plasma-channel guiding. *Nature*, 431(7008):538–541, Sep 2004.

[16] A E Pak, Ken Marsh, S F Martins, Wei Lu, W B Mori, and C Joshi. Injection and trapping of tunnel-ionized electrons into laser-produced wakes. 104(2), Jan 2010.

[17] M. Mirzaie, S Li, M Zeng, N. A. M. Hafz, M Chen, G Y Li, Q J Zhu, H Liao, T. Sokollik, F Liu, Y Y Ma, L.M Chen, Z M Sheng, and J Zhang. Demonstration of self-truncated ionization injection for GeV electron beams. *Scientific Reports*, 5(1), Oct 2015.

[18] W. Lu, M. Tzoufras, C. Joshi, F. S. Tsung, W. B. Mori, J. Vieira, R. A. Fonseca, and L. O. Silva. Generating multi-gev electron bunches using single stage laser wakefield acceleration in a 3d nonlinear regime. *Physical Review Special Topics - Accelerators and Beams*, 10(6), Jun 2007.

[19] Jan-Niclas Gruse. *Development of Laser Wakefield Accelerators*. PhD thesis, Imperial Coll., London, 2020.